

Latitude Distribution of Star-spots on the G Dwarf He 699

S.V.Jeffers¹, J.R.Barnes¹, A.C.Cameron¹

Abstract.

We analyse the latitude distribution of star-spots on the rapidly rotating G dwarf He 699. An image was reconstructed from data taken with the William Herschel Telescope on La Palma on 2000 October 08. The predominant magnetic field structure is a decentred polar spot at high latitude, with smaller low latitude features also present. This result was verified by independent reconstructions using even numbered and odd numbered spectra. This work confirms and extends that of Barnes et al. (2001, MNRAS, 326, 1057) and provides further evidence that there is a correlation between the presence of low latitude features and the amplitude of the photometric lightcurve. It is also a further step in the search for activity cycles on young G dwarfs.

1. Introduction

Star-spots are the most easily observed form of magnetic activity on cool stars with an outer convective zone. Using modern indirect imaging techniques such as Doppler Imaging combined with high precision optical photometry, it is possible to measure the lifetimes, surface brightness, latitude distributions, local rotation rates of stellar spots and any changes in these properties as the stellar magnetic cycle progresses.

The stars that display such activity are rapidly rotating, young, main sequence stars. An example of a cluster is α Persei, which is a young open cluster around its same named brightest member. The distance to α Per is 181.5 ± 22.1 pc as given by the Hipparcos parallax. It has many late-type stars with high rotation rates typically of the order of 0.5 d (Prosser 1991). This rapid rotation is present in α Per in early G to early K dwarfs. He 699 is such a G dwarf in the α Per cluster. It is a rapidly rotating G dwarf with a rotation period of 0.49 days, an equatorial $v \sin i = 93.5 \text{ km s}^{-1}$ and an inclination of 52.5° (Barnes et al. 2001). As He 699 has $m_v=11.5$, it is only with the advent of signal enhancing techniques, such as least-squares deconvolution, that it is possible to apply Doppler Imaging to determine the spot coverage of such faint stars. This was first applied to He 699 by Barnes et al. (1998).

In this paper the work of Barnes et al. (1998 & 2001) is extended by studying the star-spot distribution on the α Per member He 699, four years after the original observations.

¹The University of St Andrews

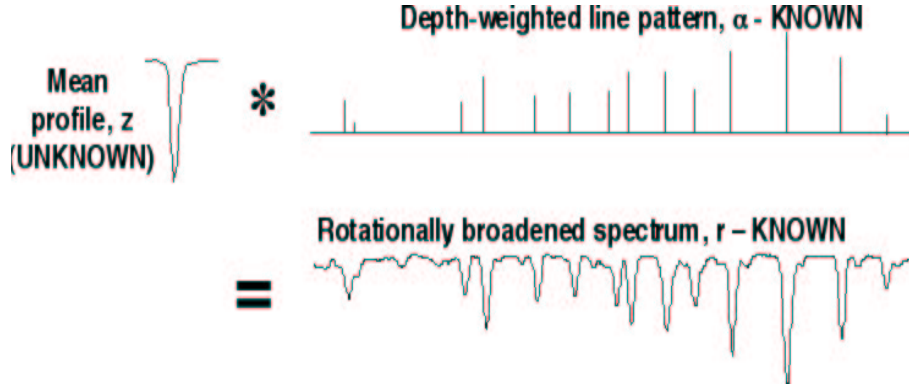


Figure 1. Schematic of the method of Least-Squares Deconvolution

2. Observations

This analysis uses a combination of spectroscopy and photometry. The spectroscopy was obtained at the 4.2m William Herschel Telescope on La Palma, on 2000 October 08. The detector was an array of two EEV CCDs, each with 2048 x 4096 13.5 μ m pixels, centered at 5000 \AA . The exposures were each of 600 s duration. Following extraction, the S:N in the continuum of the central order is 14 per pixel.

The photometry was obtained at the 0.93m James Gregory Telescope in St Andrews, on 2000 October 14, with 60 s exposures. The photometric observations were made in the V band (5450 \AA).

Here, the one dimensional echelle spectra were extracted using the Starlink ECHOMOP (Mills 1994) and FIGARO reduction packages through the automated pipeline routine. The photometric data were reduced using JGTPHOT, a software package developed for use with the James Gregory Telescope at St Andrews (Bell Hilditch & Edwin 1993).

3. Least Squares Deconvolution

As He 699 is $m_v=11.5$, it is necessary to apply the technique of least-squares deconvolution. The least-squares deconvolution (LSD) method (Donati et al. 1997) optimally uses the information content of weak lines to increase the S:N. In this analysis a gain of 44 was achieved. LSD treats the observed spectrum as a convolution of a mean profile, z , and a depth weighted line pattern, as shown in Figure 1.

The least-squares deconvolution process can be simplistically described as solving the vector equation

$$\frac{\delta\chi^2}{\delta z_k} = 0, \quad (1)$$

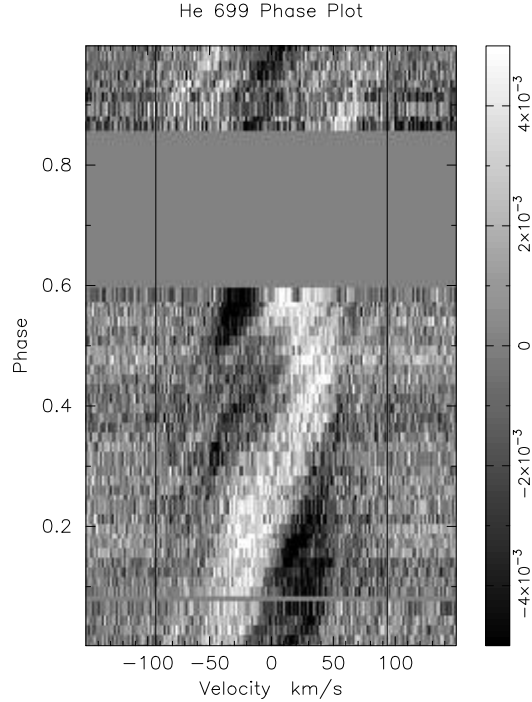


Figure 2. Time series spectra for He 699, with the mean profile subtracted. The vertical lines are at the $v\sin i$ of He 699, 93.5° .

where,

$$\chi^2 = \sum_j \frac{(r_j - \sum \alpha_{jk} z_k)^2}{\sigma_j^2} \quad (2)$$

Here z_n represents the best fitting composite profile which, when convolved with a pattern of line positions and strengths encoded in the transformation matrix α , yields an optimal fit to the observed spectrum. A more detailed mathematical explanation is given by Donati et al (1997) and Collier Cameron (2001).

The time series spectra that were produced using least-squares deconvolution are shown in Figure 2. In the times series spectra it is possible to identify low latitude spots and a more slowly varying asymmetry in the line profile that is indicative of a large, off centered structure at high latitude. This high latitude structure crosses the disc centre at approximately phase 0.25 to 0.3, coinciding closely with the photometric minimum.

4. Image Reconstruction

The maximum entropy code DOTS, (Cameron 1997, 1992 and Cameron et al. 1992) was used to reconstruct surface images of He 699 from the spectroscopic

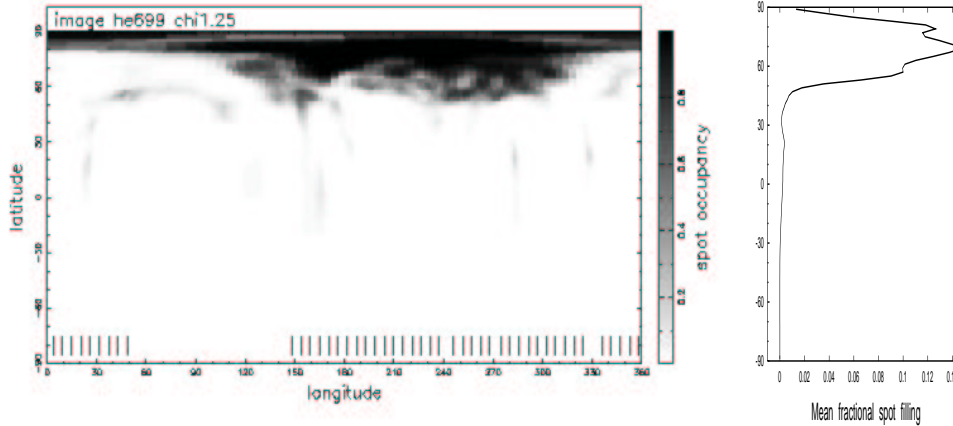


Figure 3. Maximum entropy image reconstructions for He 699, 2000 October 08. On the right, the mean fractional spot occupancy of the image as a function of latitude

line profiles and the photometric lightcurve. DOTS is based on the MEMSYS algorithm of Skilling and Bryan (1984). The stellar surface geometry model and integration scheme are described by Cameron (1992).

In this case a stellar surface grid with 90 latitude bands was used in the image reconstruction. To adjust the relative contributions of the final surface image on the spectroscopic or photometric data sets, there is a weighting factor included in DOTS.

To account for the difference in the spot and photospheric temperature, it is necessary to use two template stellar spectra. These stars are an M1 dwarf (HD 1326) with a photospheric temperature $T=3500$ K representing the spot temperature, and a G2V dwarf (HR 6847) with $T=5750$ K for the non-spotted photosphere.

5. Results and Discussion

The maximum entropy reconstructions for He 699, Figure 3, indicate clearly that the main occurrence of spot coverage on the stellar surface are at high latitudes. Also present are low latitude features. These occur at latitudes $\leq 30^\circ$ and are elongated in longitude. The reasoning behind this vertical structure is that $\dot{v} \propto \cos(\text{latitude})$ is insensitive to small changes in latitude at the equator. The entropy criterion expresses the uncertainty in longitude by smearing the image north-south at low latitudes.

The image that resulted from the cross correlation of the even numbered and odd numbered spectra is shown in Figure 4. The central vertical band in this plot signifies that there is a correlation between these two data sets.

The final reconstructed image is in good agreement with the previous study by Barnes et al.(1998 & 2001) for the same star. Barnes et al. (2001) reconstructed surface images using the same methods as in this analysis for data obtained in 1996 October and November. These images show a polar spot, and

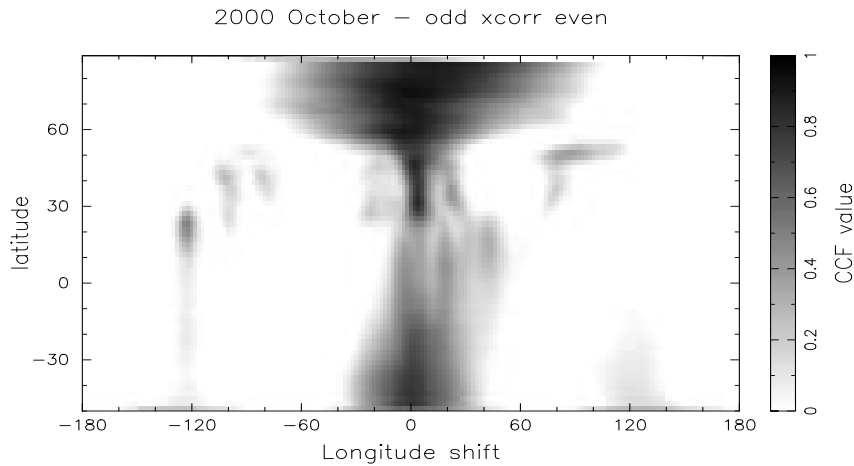


Figure 4. Image obtained from the cross correlation of the even and odd numbered spectra

a decentered polar spot respectively for each of the observations, comparing well with the results of this analysis. An interesting point of comparison between the image reconstructions is present in the low latitude spot coverage. Whereas the 1996 data sets have significant low latitude features, there is little present in the current data set. This contrast is also present in the amplitude of the photometric light curve, with the amplitude of the 1996 data set being of a factor of two greater than the amplitude of the current data set. The significance of this further verifies that there is a correlation between the presence of low latitude features and the amplitude of the photometric lightcurve.

References

- Barnes, J.R. Cameron, A.C. Unruh, Y.C. Donati, J.-F. & Hussain, G.A.J. 1998, MNRAS, 299, 904
- Barnes, J.R. Cameron, A.C. James, D.J. & Steeghs, D.I. 2001, MNRAS, 326, 1057
- Bell, S. Hilditch, R. & Edwin, R. 1993, MNRAS, 260, 478
- Cameron, A.C. 2001, Astro-Tomography. In: An International Workshop on Indirect Imaging, ed. H. Boffin, Danny Steeghs, Jan Cuypers. Lecture Notes in Physics, in press
- Cameron, A.C. 1997, MNRAS, 287, 556
- Cameron, A.C. Jeffery, C.S. & Unruh Y.C. 1992, In: Jeffery C.S., Griffen R.E.M., eds Stellar Chromospheres, Coronae and Winds. Institute of Astronomy, Cambridge, 81
- Donati, J.-F. Semel, M. Carter, B.D. & Cameron, A.C., 1997, MNRAS, 291, 658

Mills, D. 1994, Starlink User Note 152 Rutherford Appleton Laboratory
Prosser, C.F. 1991, Ph.D. thesis, Univ. of California, Santa Cruz
Skilling, J. & Bryan, R.K. 1984, MNRAS, 211, 111